Third-Order Nonlinear Optical Properties of an Ultrathin Film Containing a Porphyrin Derivative

Li Jiang,[†,‡] Fushen Lu,[†] Hongmei Li,[†] Qing Chang,[‡] Yuliang Li,*[,†] Huibiao Liu,[†] Shu Wang,[†] Yinglin Song,*[,‡] Guanglei Cui,[†] Ning Wang,[†] Xiaorong He,[†] and Daoben Zhu[†]

CAS Key Laboratory of Organic Solids, Institute of Chemistry, Chinese Academy of Sciences, Beijing 100080, P. R. China, and Department of Applied Physics, Harbin Institute of Technology, Heilongjiang 150001, P. R. China

Received: November 1, 2004; In Final Form: February 5, 2005

An ultrathin nanoscopic multilayer film has been fabricated through the electrostatic layer-by-layer self-assembly of negatively charged 5,10,15,20-tetrakis(3,4,5-trihydroxyphenyl)porphyrin (DHP) and oppositely charged polyethylenimine (PEI). UV−vis spectra showed a continuous and uniform deposition process of PEI and DHP. The film structure was characterized by small-angle X-ray diffraction measurement and AFM images. The nonlinear optical properties of ultrathin film were studied by Z-scan technique with laser duration of 8 ns at a wavelength of 532 nm. The film sample exhibited strong nonlinear saturated absorption and a self-defocusing effect. The nonlinear absorption coefficient and refractive index of the self-assembly ultrathin film are -9.7×10^{-5} m/W and -7.56×10^{-12} m^2/W, respectively.

Introduction

Third-order nonlinear optical materials are playing an important role in the technology of photonics, especially in all-optical switching, signal processing, and ultrafast optical communications.[1] Organic materials, in particular, with the structure of extensively delocalized π-electrons have received significant attention recently due to their large nonlinear optical susceptibilities, architectural flexibility, and ease of fabrication.[2,3] Current research aims to develop materials with improved and optimized nonlinear optical properties via rational design and synthesis. Among the various molecules studied, porphyrins and their derivatives have exhibited great potential application values because of their two-dimensional structures and unique electronic properties.[4−6] The nonlinear optical response of phorphyrin depends strongly on the molecular structure. It was found that hyperpolarizabilities of porphyrin molecules could be enhanced effectively through functionalization at the peripheral positions.[7−9] Various functional groups on the *meso*- or β-positions of the porphyrin can result in different nonlinear optical properties.[4,10,11]

In the past two decades, there have been a number of reports on the nonlinear optical properties of porphyrins and their derivatives based on the bulk materials.[12−16] However, it was found that the solid film materials with highly ordered molecular assemblies can exhibit extremely interesting properties including a high nonlinear optical susceptibility.[17−19] NLO properties of some porphyrin-containing thin films formed by various techniques have been investigated.[20−22] The layer-by-layer electrostatic self-assembled technique has been one of the most simple and effective methods to form orderly solid films since Decher's pioneering work in 1991.[23] By using suitably charged polyelectrolyte as counterions, charged materials of interest can be deposited to create ultrathin films that possess not only nanoscopic level structure but also important optical or electric properties.[24] So far, the NLO properties of a solid film containing porphyrin units fabricated by the electrostatic layer-by-layer technique have been seldom reported.

In this paper, a water-soluble porphyrin derivative (DHP) was synthesized by using different methods from the literature[25,26] and then an ultrathin composite film was fabricated from DHP with use of polyethylenimine (PEI) as an oppositely charged polyelectrolyte by the layer-by-layer electrostatic self-assembled technique. The NLO properties of ultrathin films containing a porphyrin unit were studied by the *Z*-scan technique.[27]

Experimental Section

Materials. Polyethylenimine (Mn = 60 000), 50 wt % solution in water, was purchased from Aldrich and used without further purification. All solvents and chemicals were used as received except dichloromethane, which was distilled from calcium hydride. The quartz slides for the UV−vis study and *Z*-scan measurement were cleaned by sonication in isopropyl alcohol and deionized water in turn for 30 min, and subsequently dried with argon. After being dipped in 5 M KOH for 1 min, the slides were rinsed with deionized water to remove residual KOH, and then dried under argon to make their surfaces sufficiently overlaid with negative charges. The quartz substrates for the small-angle X-ray diffraction study were cleaned with a solution of H_2SO_4−30% H_2O_2 (3:1, v/v) by sonication for 30 min and washed with deionized water. After drying, the slides were treated with another solution of deionized water, 30% H_2O_2 and $NH_3 \cdot H_2O$ (5:1:1, v/v/v). The slides were stored in deionized water prior to use after treatment.

Measurements. The growth of the film was monitored by Hitachi U-3010 UV−vis spectroscopy. Small-angle X-ray diffraction was carried out with a high-resolution Bruker D8 diffractormeter, using Cu Kα radiation (λ = 1.5405 Å). Atomic force microscopy (AFM) measurements were carried out in air at room temperature with a Nanoscope III instrument (Digital

* Address correspondence to this author.
[†] Chinese Academy of Sciences.
[‡] Harbin Institute of Technology.

10.1021/jp045024x CCC: $30.25
Published on Web 03/15/2005

SCHEME 1: Synthetic Route for DHP

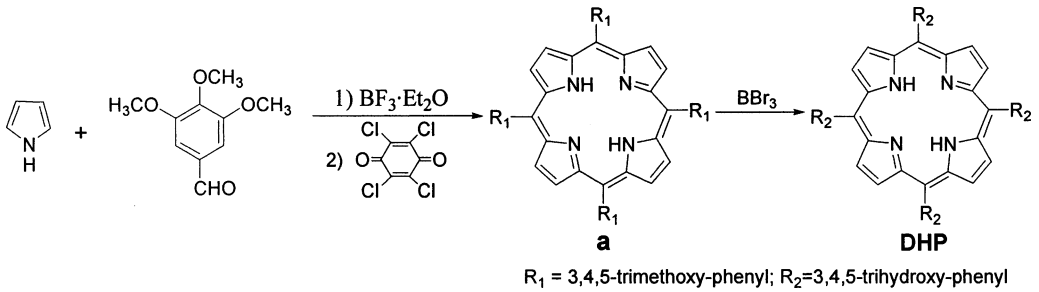

Instruments) operating in the tapping mode and AFM images were taken on mica substrates. An aqueous solution of DHP was placed in a 2-mm quartz curette for NLO measurements. The compounds are stable toward air and laser light. A frequency-doubled Q-switched Nd:YAG laser producing 8 ns (fwhm) laser pulses at 532 nm with a repetition rate of 1 Hz was used. The spatial profiles of the optical pulses were nearly Gaussian. The laser beam was focused with a 30 cm focal length focusing mirror. The incident and transmitted pulse energies were measured simultaneously with two energy detectors (Laser Precision Rjp-735), which were linked to a computer by an RS232 interface. The NLO properties of the samples were manifested by moving the samples along the axis of the incident laser irradiance beam (*Z* direction) with respect to the focal point and incident laser irradiance was kept constant. The closed-aperture curves are normalized to the open aperture curves. The linear transmission of the solution sample solution placed in the quartz cell of a thickness of 2 mm is 87% and that of the ultrathin film is 32%. The beam size of the laser pulses at the focus is 78 μm and the on-axis peak intensity at the focus ($z = 0$) is 4.06×10^7 W/cm^2 for an input energy of 36 μJ.

Synthesis of Water-Soluble Porphyrin. The general synthetic approach to the water-soluble anionic 5,10,15,20-tetrakis-(3,4,5-trihydroxyphenyl)porphyrine (DHP) was shown as Scheme 1. First, 5,10,15,20-tetrakis(3,4,5-trimethoxyphenyl)porphyrine (**a**) was prepared by condensation of 3,4,5-trimethoxybenzaldehyde and pyrrole (1:1 molar ratio) involving $(C_2H_5)_2O{\cdot}BF_3$ as a catalyst, followed by oxidation with tetrachloro-*p*-benzoquinone in $CHCl_3$.[28] Then, at −78 °C, excessive BBr_3 (50:1, molar ratio) was added dropwise into the solution of compound **a** in CH_2Cl_2. After the mixture was stirred for 24 h at room temperature under nitrogen, the DHP was afforded as a dark solid (yield: 29%). ^{1}H NMR (300 MHz, CD_3OD) δ 9.23(br s, 8H), 8.97 (s, 8H), 8.84 (br s, 4H), 7.20 (s, 8H), −2.89 (br s, 2H). FT-IR (KBr) ν 3423, 1603, 1532, 1473, 1357, 1306, 1230, 1041, 833, 744, 651. MALDI-TOF MS *m*/*z* 807 $[M + H]^+$.

Film Growth and Characterization. Layer-by-layer deposition on quartz substrates was carried out by sequential treatment of the substrates with solutions of positive charged PEI and negatively charged DHP in turn. DHP was dissolved in deionized water at a concentration of 1 mg/mL, using NaOH solution to adjust the pH value to 9, and PEI was diluted to 5 wt % of solution. The cleaned substrates were alternately dipped in the cationic and anionic solutions for 5 min, respectively (Scheme 2). After each deposition step, the surface of the self-assembled film was washed with deionized water and dried with a stream of argon gas. All of the experiments were carried out at room temperature.

Results and Discussion

UV−vis absorption spectroscopy was used to monitor the electrostatic self-assembly process of the PEI/DHP multilayer

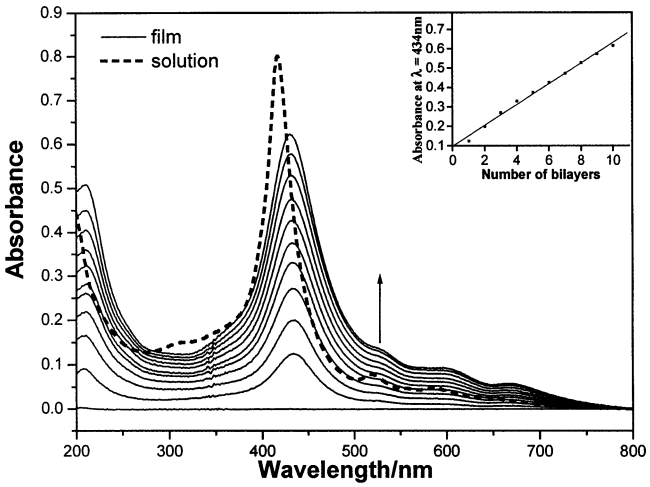

Figure 1. Absorption spectra of PEI/DHP multilayer films with different numbers of bilayers. Inset: The relationship of the absorbance and the number of bilayers.

SCHEME 2: The Procedure for Fabrication of the PEI and DHP Film by Alternate Absorption

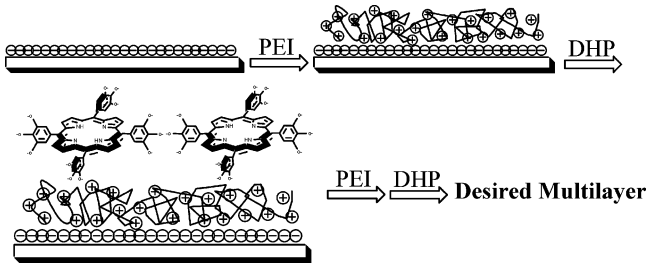

film. The absorption spectra of the film sample are shown in Figure 1. The spectra exhibit a clear strong absorption around 434 nm, which is the characteristic Soret band of porphyrins. In aqueous solution, the $\pi-\pi^*$ absorption maximum was observed at 418 nm. The obvious red shift for the absorption of the multilayer film can be explained as the strong interaction between individual molecules in the densely packed films.[29] A series of weaker Q-bands ranging from 500 to 800 nm can also be seen in Figure 1. In addition, an overall broadening of the absorption spectra was noted compared with that of DHP in water. The broadening is probably due to the strong interaction between individual dyad molecules and light scattering in the densely packed films.[30] By plotting the optical density at 434 nm against the number of bialyers, a good linear relationship can be obtained, as shown in the inset spectrum in Figure 1. A linear fit yields an average increase of the absorption intensity of 0.0553 (correlation coefficient $R = 0.997$) per bilayer, indicating a stepwise and regular growth process.

Further evidence for the multilayer structure is provided by the small-angle X-ray diffraction study. Figure 2 shows the X-ray diffraction pattern of a 30-bilayer film of PEI and DHP

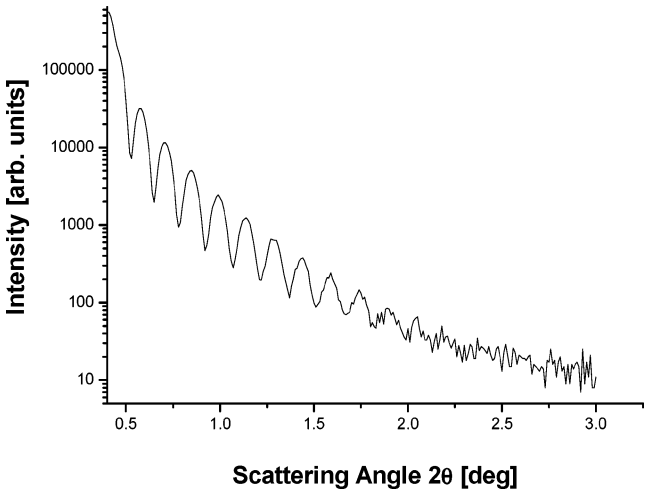

Figure 2. Small-angle X-ray diffraction pattern of a 30-bilayer film of PEI and DHP.

prepared on quartz substrates. The X-ray curve reveals a series of Kiessig fringes, which suggested that the PEI/DHP layer-by-layer film is uniform and flat. The total thickness of the film was calculated to be about 62 nm from the spacing of the peaks.[23] Since the UV−vis spectra demonstrated that the thickness of the film increased uniformly with the number of layers, the average thickness of one bilayer can be calculated to be about 2.1 nm.

The AFM images should provide more detailed information on the domain structure and the surface roughness. The mica surface is ideal for the AFM because it is not only atomically flat but also carries a negative charge (K^+ counterion), which is necessary for the electrostatic assembly. The tapping-mode AFM image of the PEI/DHP film and the corresponding 3D image are shown in Figure 3. The morphologies of the PEI/DHP film present a dispersed grained structure with an average diameter of about 100 nm. The height variation of the surface is about 15 nm and the mean interface roughness is measured to be 1.6 nm. From the image, we can see the stacked aggregates formed during the adsorption process. AFM images, together with the linear increase of absorption in UV−vis spectra and X-ray diffraction study, suggest that the self-assembly of the PEI/DHP ultrathin film is moderately uniform.

Nonlinear Optical Measurement. The *Z*-scan technique is a single-beam method for measuring the optical nonlinearities through detecting the far-field sample transmittance of a focused Gaussian beam as a function of sample position (*z*). This method provides a direct measurement of nonlinear absorption and refraction along with the sign of nonlinearity. The sign of the nonlinearity is an important parameter for practical application of optical signal processing devices. This information cannot be obtained by the other commonly used techniques such as degenerate four-wave mixing (DFWM) and third-harmonic generation (THG). In the *Z*-scan measurement, the intensity-dependent transmission of the sample measured without an aperture (open aperture scan) gives information on purely absorptive nonlinearity whereas the apertured scan (closed aperture) contains the information of both the absorptive and dispersive nonlinearities. The ratio of the normalized closed aperture and open aperture scans generates a *Z*-scan due to the purely dispersive nonlinearity.

We first performed a *Z*-scan measurement on a standard sample carbon disulfide (CS_2) in a quartz cell with 1 mm thickness (shown in Figure 4). The nonlinear refractive index n_2 for CS_2 was measured to be 5.7×10^{-17} m^2/W (2.21×10^{-10} esu), which is very close to the reported value.[27,31] The vacant quartz substrates and quartz cells used in our experiments exhibit very weak optical nonlinearities and their effects on the experimental results can be neglected.

The NLO properties of the 20-bilayer film of DHP and PEI were investigated with 532 nm laser pulses of 8 ns duration by using the normalized energy transmission *Z*-scan technique. In addition, the 0.33 mg/mL solution of DHP in deionized water is investigated under the same experimental condition as the film sample to compare the NLO difference between solid film and solution (PEI having no optical nonlinearities). The nonlinear absorption component of the samples is evaluated under an open-aperture configuration. The NLO absorption data obtained under the condition used in this study can be well described by eq 1,[32] which describes a third-order NLO absorptive process.

$$T(z) = \frac{1}{\sqrt{\pi}q(z)}\int_{-\infty}^{\infty} \ln[1 + q(z)]e^{-\tau^2}\,d\tau$$

$$q(z) = \alpha_2^{\text{eff}} I(z)\frac{1 - e^{-\alpha_0 L}}{\alpha_0} \qquad (1)$$

Where α_0 and α_2 are linear and effective third-order NLO absorptive coefficients, τ is the time, and L is the optical path. Light transmittance (T) is a function of the sample's Z position (with respect to the focal point at $Z = 0$). The open aperture *Z*-scan curves of both the film on the quartz substrate and the

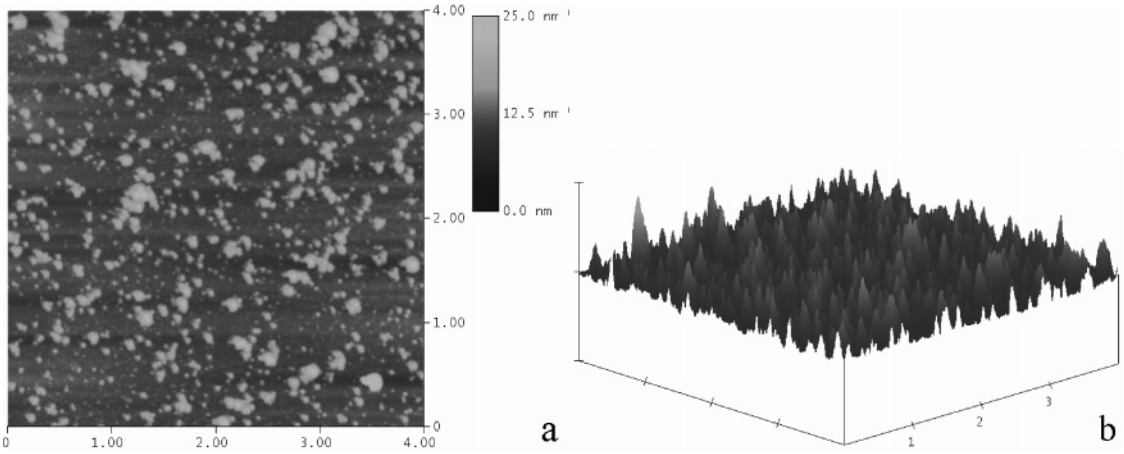

Figure 3. The tapping-mode AFM image of the PEI/DHP 10-bilayer film on mica in the 4×4 μm region (a) and the corresponding 3D image (b).

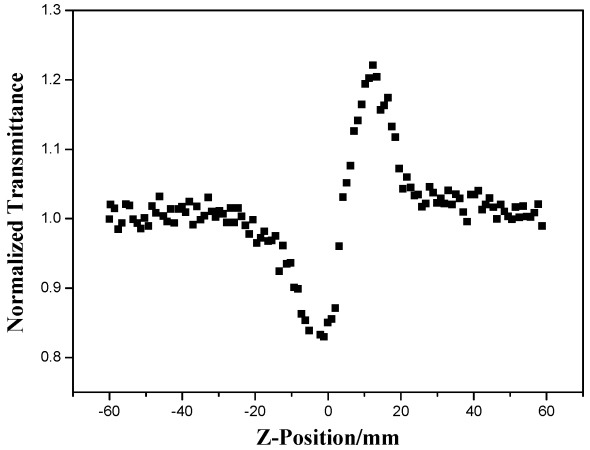

Figure 4. *Z*-scan curve of a standard sample of carbon disulfide (CS_2) in a 1 mm length quartz cell under the closed-aperture configuration.

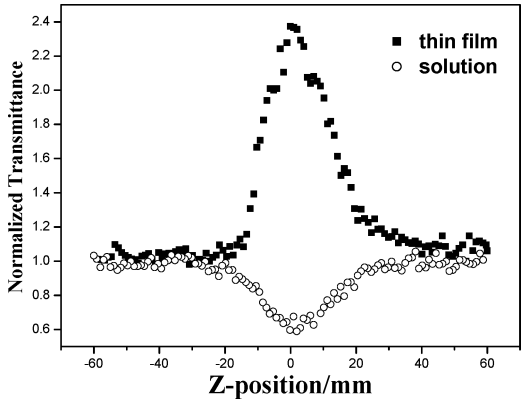

Figure 5. *Z*-scan data for the PEI/DHP 20-bilayer film (squares) and DHP in 0.33 mg/mL solution (circles) collected under an open aperture configuration.

solution sample in the quartz cell at 532 nm are shown in Figure 5. The samples were scanned 60 mm on either side of the focus. For the film sample, the normalized power transmittance increases at the focus by nearly 2.3 times compared to that of the low power transmittance, indicating a very strong saturated absorber behavior. The DHP solution, on the contrary, exhibits weaker reverse saturated absorption. The nonlinear absorption of the solutions of porphyrin derivatives is well-known to result from excited-state absorption.[33,34] For the ultrathin film with nanostructure, the surface effect is crucial to lead the saturated absorption.[35] The effect of resonance enhancement can be neglected though the absorption at 532 nm, which lies on the shoulder of the main linear absorption band for the nonlinear absorption both in water and in film, is relatively small. The nonlinear absorption coefficient α_2 of the film is -9.7×10^{-5} m/W and that of the solution is 4.61×10^{-10} m/W according to respective experimental curves.

The NLO refractive effects are assessed by dividing the normalized *Z*-scan data obtained under the closed aperture configuration by those under the open-aperture configuration. An effective third-order NLO refractive index n_2 can be derived from the difference between normalized transmittance values at valley and peak positions (ΔT_{v-p}), using eq 2.[32,36]

$$n_2 = \frac{\lambda \alpha_0}{0.812\pi I(1 - e^{-\alpha_0 L})} \Delta T_{v-p} \qquad (2)$$

Where ΔT_{v-p} is the difference between normalized transmittance values at valley and peak portions, I is the peak irradiation intensity at focus, and λ is the wavelength of the laser.

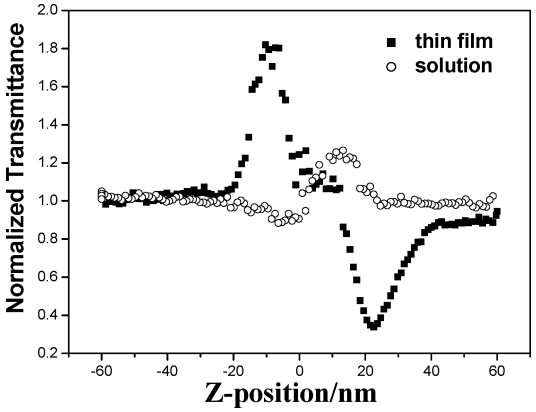

Figure 6. Normalized closed-aperture *Z*-scan curve of a 20-bilayer film sample of PEI/DHP (squares) and a 0.33 mg/mL solution of DHP (circles) under the closed-aperture configuration.

Figure 6 presents the typical NLO refractive data for the film sample and the solution sample. The peak−valley pattern of the normalized transmittance curve (shown in solid squares) obtained under the closed-aperture configuration indicates that the PEI/DHP film has a negative sign for the nonlinear refraction and exhibits a strong self-defocusing behavior. The peak position is at −10.5 mm before the focus and the valley position is at 20.5 mm behind the focus. The peak−valley position of the normalized transmissions is not symmetrical with respect to the focus ($Z = 0$). This asymmetry is supposed to be induced by nonlinear scattering from the formation of scattering centers.[37,38] It can be seen from Figure 6 that the difference between normalized transmittance values at peak and valley portions, ΔT_{v-p}, is 1.48. The effective third-order refractive index n_2 of the 20-bilayer film is calculated to be -7.56×10^{-12} m^2/W by eq 2. On the other hand, the peak−valley pattern of the normalized transmittance curve (shown in open circles) indicates the DHP solution possesses a positive sign for the nonlinear refraction and exhibits self-focusing behavior with $\Delta T_{v-p} = 0.38$. The effective third-order nonlinear refractive index n_2 of the DHP solution is 3.47×10^{-17} m^2/W.

From the above results, it can be easily seen that the self-assembled solid film can enhance effectively the optical nonlinearities of organic materials. This indeed provides a convenient approach to exploit more NLO solid materials with large nonlinear response.

Conclusion

A novel ultrathin multilayer film with well-ordered nanoscopic structure, containing DHP associated with PEI as oppositely charged polyelectrolyte, has been fabricated by the layer-by-layer electrostatic self-assembled technique. The nonlinear response of the 20-bilayer film has been probed with use of the *Z*-scan technique. Experimental results indicate the PEI/DHP film possesses strong saturated absorptive and self-defocusing nonlinearities. Moreover, the third-order optical nonlinearities of the ultrathin film are clearly better than that of DHP in solution. Further investigation of the mechanism resulting in the phenomenon is still underway. The novel ultrathin film architecture exhibits great potential applications for new optical devices.

Acknowledgment. The authors acknowledge the National Natural Science Foundation of China (50172013, 50372070, 20418001, 20473102, 20131040) for support.

References and Notes

(1) *Handbooks of Optics IV, Fiber Optics & Nonlinear Optics*, 2nd ed.; Bass, M., Enoch, J. M., Stryland, E. W. V., Wolfe, W. L., Eds.; Mcgraw-Hill: New York, 2001.

(2) Bredas, J. L.; Adant, C.; Tackx, P.; Petersoons, A.; Pierce, B. M. *Chem. Rev.* **1994**, *94*, 243.

(3) Nalwa, H. S. *Adv. Mater.* **1993**, *5*, 341.

(4) Anderson, H. L.; Martin, S. J.; Bradeley, D. D. C. *Angew. Chem., Int. Ed. Engl.* **1994**, *33*, 655.

(5) Nalwa, H. S.; KaKuta, A.; Mukoh, A. *Chem. Phys. Lett.* **1993**, *203*, 109.

(6) Nalwa, H. S.; Kakuta, A.; Mukoh, A. *J. Phys. Chem.* **1993**, *97*, 10515.

(7) Bezerra, A. G., Jr.; Borissevitch, I. E.; de Araujo, R. E.; Gomes, A. S. L.; de Araújo, C. B. *Chem. Phys. Lett.* **2000**, *318*, 511.

(8) Rao, S. V.; Srinivas, N. K. M. N.; Rao, D. N.; Giribabu, L.; Maiya, B. G.; Philip, R.; Kumar, G. R. *Opt. Commun.* **2000**, *182*, 255.

(9) Kuebler, S. M.; Denning, R. G.; Anderson, H. L. *J. Am. Chem. Soc.* **2000**, *122*, 339.

(10) Albert, I. D. L.; Marks, T. J.; Ratner, M. A. *Chem. Mater.* **1998**, *10*, 753.

(11) Belijonne, D.; O'keefe, G. E.; Hamer, P. J.; Friend, R. H.; Anderson, H. L.; Brédas, J. L. *J. Chem. Phys.* **1997**, *106*, 9439.

(12) Collman, J. P.; Kendall, J. L.; Chen, J. L.; Eberspacher, T. A. *Inorg. Chem.* **1997**, *36*, 5603.

(13) McEwan, K.; Lewis, K.; Yang, G.-Y.; Chng, L.-L.; Lee, Y.-W.; Lau, W.-P.; Lai, K.-S. *Adv. Funct. Mater.* **2003**, *13*, 863.

(14) Kuebler, S. M.; Denning, R. G.; Anderson, H. L. *J. Am. Chem. Soc.* **2001**, *124*, 22.

(15) Terazima, M.; Shimizu, H.; Osukab, A. *J. Appl. Phys.* **1997**, *81*, 2946.

(16) Anderson, H. L.; Martin, S. J.; Bradley, Do. D. C. *Angew. Chem., Int. Ed. Engl.* **1994**, *33*, 655.

(17) Li, D.; Ratner, M. A.; Marks, T. J.; Zhang, C.; Yang, J.; Wang, G. K. *J. Am. Chem. Soc.* **1990**, *112*, 7389.

(18) Li, D.; Marks, T. J.; Zhang, C.; Yang, J.; Wang, G. K. *Proc. SPIE-Int. Soc. Opr. Eng.* **1990**, *1337*, 341.

(19) Li, D.; Marks, T. J.; Zhang, C.; Wang, G. K. *Synth. Met.* **1991**, *41*−*43*, 3157.

(20) Levy, P. M.; Ounadjela, K.; Wang, Y.; Sommers, C. B.; Fert, A. *J. Appl. Phys.* **1990**, *67*, 5914.

(21) Wen, L.; Li, M.; Schlenoff, J. B. *J. Am. Chem. Soc*, **1997**, *119*, 7726.

(22) Norwood, R. A.; Sounik, J. R. *Appl. Phys. Lett.* **1992**, *60*, 295.

(23) Decher, G.; Hong, J. D.; Schmitt, J. *Thin Solid Films* **1992**, *210*−*211*, 831.

(24) Decher, G. *Science* **1997**, *277*, 1232.

(25) Alberry, W. J.; Bartlett, P. N.; Jones, C. C.; Milgrom, L. R. *J. Chem. Res., Synop.* **1985**, *364*, 3801.

(26) Bonar-Law, P. R. *J. Org. Chem.* **1996**, *61*, 3623.

(27) Sheik-Bahae, M.; Said, A. A.; Wei, T. H.; Hagan, D. J.; Vanstryland, A. W. *IEEE J. Quantum Electron.* **1990**, *26*, 760.

(28) Lindsey, J. S.; Wagner, R. W. *J. Org. Chem.* **1989**, *54*, 828.

(29) Li, H. M.; Li, Y. L.; Zhai, J.; Cui, G. L.; Liu, H. B.; Xiao, S. Q.; Liu, Y.; Lu, F. S.; Jiang, L.; Zhu, D. B. *Chem. Eur. J.*, **2003**, *9*, 6031.

(30) Guldi, D. M.; Pellarini, F.; Prato, M.; Granito, C.; Troisi, L. *Nano Lett.* **2002**, *2*, 965.

(31) Toda, H.; Verber, C. M. *Opt. Lett.* **1992**, *17*, 1376.

(32) Zhang, C.; Song, Y. L.; Xu, Y.; Fun, H. K.; Fang, G. Y.; Wang, Y. X.; Xin, X. Q. *J. Chem. Soc., Dalton Trans.* **2000**, 2823.

(33) Liu, Z.; Tian, J.; Zang, W.; Zhou, W.; Song, F.; Zhang, C.; Zheng, J.; Xu, H. *Opt. Lett.* **2004**, *29*, 1099.

(34) McEwan, K.; Lewis, K.; Yang, G.; Chng, L.; Lee, Y.; Lau, W.; Lai, K. *Adv. Funct. Mater.* **2003**, *13*, 863.

(35) Ai, X.; Jin, R.; Ge, C.; Wang, J.; Zou, Y.; Zhou, X.; Xiao, X. *J. Chem. Phys.* **1997**, *106*, 3387.

(36) Hou, H. W.; Wei, Y. L.; Song, Y. L.; Zhu, Y.; Li, L. K.; Fan, Y. T. *J. Mater. Chem.* **2002**, *12*, 838.

(37) Murzina, T. V.; Nikulin, A. A.; Aktsipetrov, O. A.; Ostrander, J. W.; Mamedov, A. A.; Kotov, N. A.; Devillers, M. A. C.; Roark, J. *Appl. Phys. Lett.* **2001**, *79*, 1309.

(38) Konorov, S. O.; Sidorov-Biryukov, D. A.; Bugar, I.; Kovac, J.; Fornarini, L.; Carpanese, M.; Avella, M.; Errico, M. E.; Chorvat, D.; Kovac, J.; Fantoni, R.; Chorvat, D.; Zheltikov, A. M. *Appl. Phys. B*: *Lasers Opt.* **2004**, *78*, 73.